Non-contact surface resistivity tester for materials from 10^6 to 10^{11} Ω

Kazuki Numayama[1], Toshiyuki Sugimoto[1], Koichi Taguchi[2]
[1] Dept. of Electrical Engineering
Yamagata University
phone: (+81) 238-26-3280
e-mail: toshi@yz.yamagata-u.ac.jp

[2] NAPSON CORPORATION
phone: (+81) 43-205-5301
e-mail: k-taguchi@napson.co.jp

Abstract—**Surface resistivity is one of the most important properties in determining the electrostatic behavior of materials. We have previously developed a non-contact surface resistivity tester that uses surface potential rise time measurements along with corona charging. The system was used to successfully measure surface resistivities greater than 10^9 Ω. Because the lower limit of the rise time measurement was intrinsically determined by the response time of the surface voltmeter, it is difficult to extend the measurable range to lower than 10^9 Ω. In this study, a non-contact surface resistivity tester for materials from 10^6 to 10^{11} Ω was developed using a grid-type charge elimination apparatus, in addition to a corona charger and a surface voltmeter. The purpose of this design was to make both charging and non-charging spots on a test sample, which resulted in a steady current flow between the two spots. The steady surface potential between the two spots was measured without the influence of the surface voltmeter response time. The steady potential was determined to be a function of the surface resistivity in the range of 10^6 to 10^{11} Ω by solving an equivalent circuit model. The measured surface potential was in agreement with the surface resistivity from 10^6 to 10^{11} Ω, as predicted by the circuit model.**

I. Introduction

Surface resistivity is important to grasp the electrostatic properties of materials. Surface resistivity is categorized into three groups depending on the electrostatics behavior: conductive ($<10^5$ Ω), dissipative (between 10^5 and 10^{12} Ω), and insulative ($>10^{12}$ Ω) [1]. As in IEC 60093 [2], two concentric electrodes are applied to a test surface and the leakage current flowing through the two electrodes is measured. However, this measurement principle requires perfect contact of the electrodes to the sample, which makes it difficult to measure materials such as thin films, powders, particles, or wet coatings. A non-contact measurement should be adopted to measure such materials. Surface potential rise time [3] or decay time [4-7] measurement for a sample, followed by corona charging of the test surface, is one of the non-contact methods.

Typical surface potential rise time measurement systems include a corona charger to charge up the sample and a surface voltmeter to measure the surface potential. The measured rise time shows how quickly the static charge on the sample propagates through its surface. However, this is difficult to predict for materials with surface resistivities less than $10^9\,\Omega$ because the time variation of the surface potential is too quick to measure using a surface voltmeter [3].

We have developed a non-contact tester to measure the surface resistivity from 10^6 to $10^{11}\,\Omega$ without the influence of the surface voltmeter response time. This measurement system includes a charge elimination apparatus and a rise time measurement system (corona charger and surface voltmeter). The measurable range can be theoretically predicted from 10^6 to $10^{11}\,\Omega$. A prototype tester model using this method was prepared, and the experimental and simulated results are compared.

II. BASIC CONCEPT

A. Rise time measurement

Fig. 1 shows the basic concept of the non-contact surface resistivity tester for insulative materials higher than $10^9\,\Omega$ [3]. This method measures how quickly the surface charge on the test sample propagates through the surface. The grounded probe is composed of a corona charger and a surface voltmeter. The corona charger includes a needle electrode connected with a high dc voltage source, V_0. The distance between the tip of needle electrode and the test sample is denoted as d. The surface of the test sample is partly charged by the corona ions that arrive at the surface close to the needle, which is defined as the charging zone. The surface charge propagates over the surface at a rate that depends on the surface resistivity of the sample, due to the potential difference between the charging zone and the surrounding area. Propagation of the surface charge can be detected by the surface voltmeter. If the rise time of the surface potential is measured, then the surface resistivity can be transferred by the rise time for samples with known surface resistivity. The surface potential detection area is defined as the measurement zone.
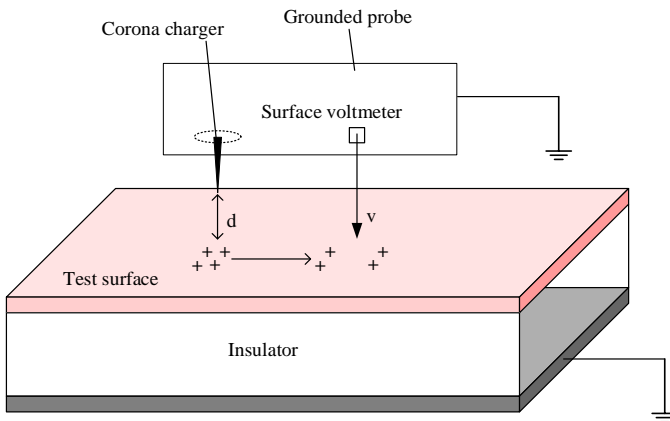
Fig. 1. Schematic showing the concept of the rise time measurement.

B. 1D equivalent circuit for rise time measurement

Fig. 2 shows the equivalent distributed element model to explain the concept of the rise time measurement. The test surface is regarded as a series of unit-length resistance R_S. An air gap exists between the grounded probe and the test surface; therefore, the capacitance and conductance should be taken into account. The unit-length capacitance and conductance are defined as C_1 and G_v, respectively. In addition, the unit-length capacitance C_0 is defined due to a stray capacitance between the test surface and the grounded materials such a desk and a grounded cable. The equivalent circuit is composed of a ladder structure of R_s, G_v, C_0, and C_1, as shown in Fig. 2. In the charging zone, the supplied ions provide the surface potential V_0.
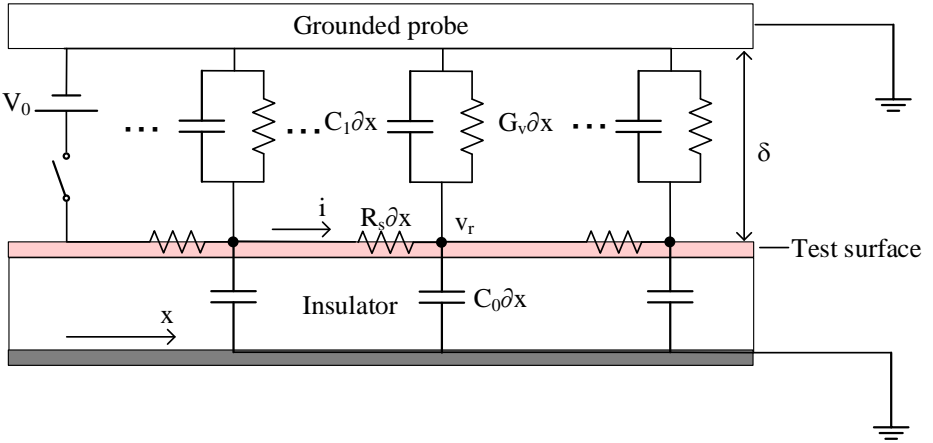
Fig. 2. Equivalent distributed element model.

C. Governing equations for the rise time measurement

Assuming that the potential and current distribution of the equivalent circuit at the measurement zone is a function of only the distance from the charging zone x and the time t, the Kirchhoff equations for differential length are given as follows:

$$\begin{cases} \dfrac{\partial v_r}{\partial x} = -R_s i \\ \dfrac{\partial i}{\partial x} = -G_v v_r - (C_0 + C_1)\dfrac{\partial v_r}{\partial t} \end{cases} \tag{1}$$

where v_r and i are the potential and current for distance x at time t, respectively, as shown in Fig. 2. The final partial differential equation for the potential v_r becomes

$$\frac{\partial^2 v_r}{\partial x^2} - R_s G_v v_r - R_s(C_0 + C_1)\frac{\partial v_r}{\partial t} = 0. \tag{2}$$

For the lower surface resistivity range, the second term on the left side of (2) can be neglected because $R_s G_v$ is negligibly small, so that

$$\frac{\partial^2 v_r}{\partial x^2} - R_s(C_0 + C_1)\frac{\partial v_r}{\partial t} = 0. \tag{3}$$

The solution of (3) at the boundary condition of $v_r(0, t) = V_0$ is given by

$$v_r(x,t) = V_0\left(1 - \mathrm{erf}\left(\sqrt{\frac{R_s(C_0 + C_1)}{4t}}\,x\right)\right) = V_0\mathrm{erfc}\left(\sqrt{\frac{R_s(C_0 + C_1)}{4t}}\,x\right) \tag{4}$$

where erf is an error function and erfc is a complementary error function. The surface potential v_r is dependent on the resistance R_s, which is proportional to the surface resistivity, the potential measurement position x, the measurement time t, and the capacitances C_0 and C_1. C_1 is always a constant because it is determined by the probe configuration. On the other hand, C_0 is not always a constant but is dependent on the sample size; therefore, C_0 can be a function of the sample size. The time variation of the surface voltage may thus be dependent on the sample size, as discussed later.

D. Steady state potential measurement for extension of the measurable range

Fig. 3 shows the basic concept of the steady surface potential measurement to extend the measurable surface resistivity range. This system includes a corona charger, a charge eliminator, and a surface voltmeter. The corona charger has a needle electrode connected with a high positive dc voltage V_+. The charge eliminator is composed of a needle electrode connected with a high negative dc voltage V_- and a grounded grid electrode. As with the transient measurement, corona ions are supplied to the test surface. However, the surface potential of the charging zone is lower than V_+ under steady state measurement because there is a voltage drop between the charging needle electrode and the test surface due to the non-linear corona resistance R_c. R_c has a current-voltage (I-V) characteristic given by

$$i_c = K(v_c - v_h)^2 \tag{5}$$

where v_c is the potential difference between V_+ and the charging zone, i_c is the current flowing through the sample, v_h is the corona onset voltage, and K is a constant.

The charge eliminator supplies the charge eliminating zone of the test surface with negative ions, which results in a steady current flow between the charging zone and the elimination zone. R_b is defined as the volume resistance between the grid electrode and the test surface.

Fig. 3 shows the equivalent circuit used to describe the concept of the steady state surface potential measurement. The surface resistance R is divided into two resistances, R_1 and R_2. R_1 is the resistance between the charging zone and the measurement zone. R_2 is the resistance between the measurement zone and the charge eliminating zone. R, R_1, and R_2 have a relationship given by

$$\begin{cases} R_1 + R_2 = R \\ R_1 = AR_2 \end{cases} \tag{6}$$

where A is a constant determined by the position of the surface voltmeter (as shown later in Fig. 5). Fig. 3 shows a voltage-divide circuit; therefore, the steady state surface potential V_{std} can be calculated as

$$V_{\mathrm{std}} = \frac{R_2 + R_b}{R_c + R_1 + R_2 + R_b}V_+ = \frac{\dfrac{A}{1+A}R + R_b}{R_c + R + R_b}V_+. \tag{7}$$

The steady surface voltage V_{std} can be measured with a surface voltmeter and the surface resistance is calculated using equation (7). To convert the surface resistance calculated to the surface resistivity, a conversion coefficient determined by the probe configuration is used.
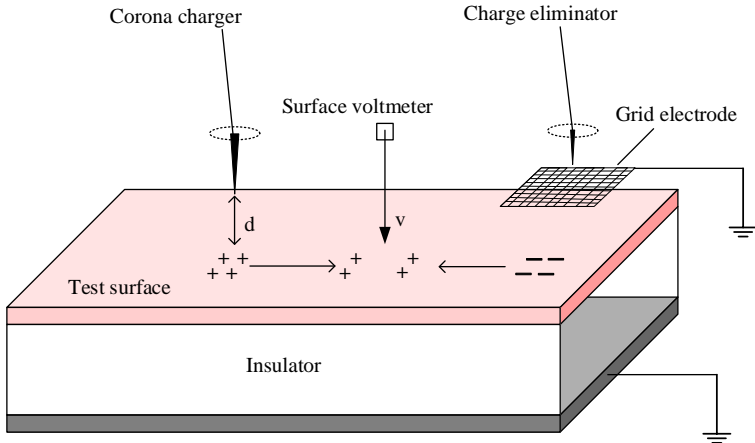
Fig. 3. Schematic illustration of the basic concept of the steady state potential measurement.
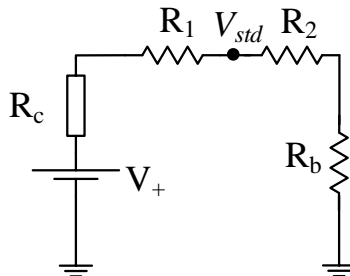
Fig. 4. Equivalent circuit used to determine V_{std}.

III. EXPERIMENTAL SETUP

A. Charging electrodes with charge eliminator

Fig. 5 shows a schematic diagram of a charging corona needle electrode and a needle electrode with a charge eliminator. A high positive dc high voltage of +3.7 kV is applied to the charging corona electrode. The diameter of the needle electrode is 1.02 mm, and the tip is sharp with a diameter of 20 μm. The charging needle electrode is placed over the test sample with a gap of $d_c = 5$ mm. The charge eliminator is composed of negative corona needle electrodes and a grounded grid electrode with 2 mm spacing. The distance between the grid and the sample is $d_g = 1$ mm. A high negative dc voltage of -4.3 kV is applied to the negative corona electrode. The sample is placed above a grounded plate with a gap of d_p.
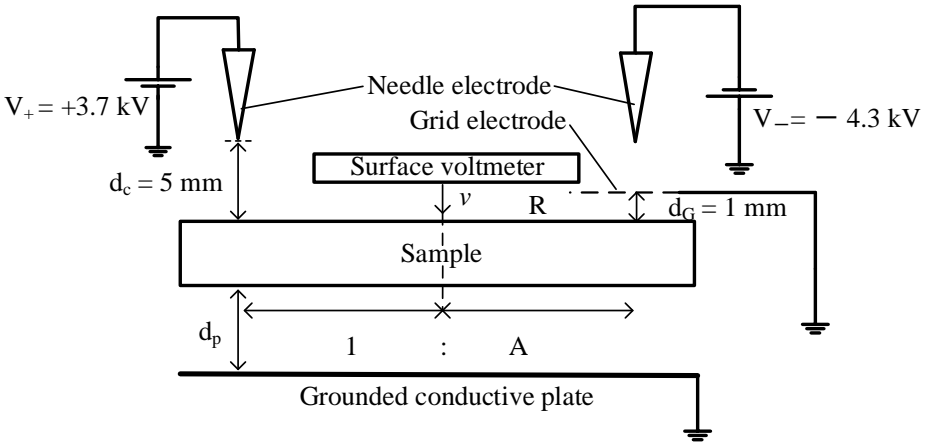
Fig. 5. Experimental setup.

B. Probe used in the measurement

The main body of the probe shown in Fig. 6 was made with a 3D printer using acrylonitrile butadiene styrene (ABS) polymer as a material. Almost all of the surface of the body is coated with a grounded conductive material, except around the electrodes. The surface voltmeter (SMC, IZD10-110), charging corona needle electrode, and charge elimination apparatus are inserted into the body. The surface voltmeter and the electrodes are separated, so that the potential of the needle electrodes does not affect the surface potential measurement.

|(a) Side view | (b) Bottom view |
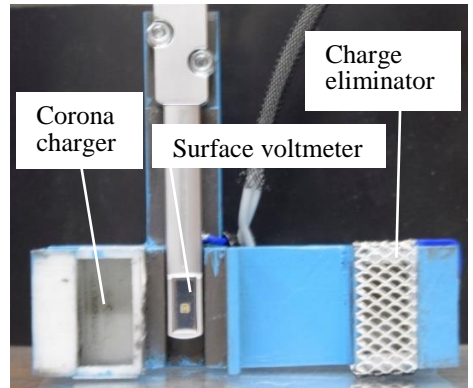
Fig. 6. Probe with the surface voltmeter, corona charger, and charge eliminator.

C. Test materials

Table 1 lists the samples tested in this investigation. The surface resistivity was measured using a commercial resistivity tester (Trek, Model 152) with electrode contact. A is a stainless steel plate, which is used as a conductive surface. B and G are high-resistivity glass samples, where the surface resistivities are adjusted by coating a

dissipative material layer. C is a glass plate coated with an n+a Si semiconductor. An antistatic spray (Showa, SB-8) is applied to acrylic plates E-1 and E-2. The major difference between E-1 and E-2 is the plate size. F is a conductive rubber sheet for the purpose of eliminating static charge.

TABLE 1: PREPARED SAMPLES

Sample	Material	Surface resistivity [Ω]	Size [mm^2]
A	Stainless steel	0	50×150
B	Glass + polymer	5.0×10^5	150×150
C	Glass + n+a Si	3.6×10^8	100×190
D	Acrylic + antistatic spray	4.0×10^9	220×180
E-1	Acrylic + antistatic spray	1.4×10^{10}	100×180
E-2	Acrylic + antistatic spray	1.3×10^{10}	220×180
F	Conductive rubber	2.9×10^{11}	90×200
G	Glass + polymer	3.0×10^{12}	200×200

D. Experiments

1) Steady surface potential measurement followed by rise time measurement

A high voltage of $V_+ = +3.7$ kV was gradually applied to the corona charging needle electrode at $t = 0$ s and a rate of 4.0 kV/s. After one second, V_+ reached 3.7 kV, a negative high voltage of -4.3 kV was applied to the negative corona needle electrode, and charge elimination started.

Equation (4) shows that the transient response of the surface potential measured is dependent on C_0, which is proportional to the sample size. To confirm this, the two samples E-1 and E-2 were prepared, then the time variations of the surface potential were measured for the samples. The distance between the sample and the grounded plate d_p is 2 mm, so that the stray capacitance C_0 was made to be larger than C_1.

After a transient process, the surface potential v was a steady value, defined as V_{std}. The experiments were conducted in relatively stable climatic conditions with relative humidity RH = 27% and temperature T = 21 °C.

2) Steady surface potential V_{std} dependence on the surface resistivity

The surface resistivity can be calculated from V_{std} using equation (7). To obtain a calibration curve, samples A-G with resistivities from 0 to 10^{12} Ω were measured in the same way as described in *1*). The grounded plate was removed to make C_0 lower.

IV. RESULTS & DISCUSSION

A. Time variation of surface potential

Fig. 7 shows the time variation of the surface potential for each sample. Before the charge elimination, all the potentials increased with time. Higher surface resistivity resulted in longer rise times, as predicted by equation (4). The increase in the surface potential before the charge elimination is considered to be caused by the continuous ion supply to the test surface below the corona charging electrode and the propagation of the surface charge to where the surface voltmeter was located. After charge elimination started, all the potentials, except that for G, decreased rapidly and reached the steady state surface potential, V_{std}.

Fig. 8 shows the surface potential for E-1 and E-2 with different sizes. Both E-1 and E-2 had almost the same V_{std} at t = 8 s because both samples have similar surface resistivities of $1.3\text{-}1.4 \times 10^{10}$ Ω. However, there is a clear size dependence on the rise time between E-1 and E-2. This diffirence of the rise time can be calculated by equation (4) and is dependent on C_0. The value of C_0 is proportional to the sample size. Thus, E-2 had a larger C_0 than that of E-1, which suggests that the rise time measurement has size dependence for a certain sensitive range around 10^{10} Ω. On the other hand, steady potential measurement was not influenced by the sample size because capacitance coupling does not appear in the dc equivalent circuit shown in Fig. 4 and equation (7).

B. Steady surface potential V_{std} dependence on the surface resistivity

The time required to obtain V_{std} is less than 1 s, except for G, where the charge supply from the charging zone and the charge elimination zone are balanced. If the surface resistivity is sufficiently high, as with G (categorized as an insulator), then the motion of charge become significantly slow and the charge eliminator does not work, as in Fig. 7.

V_{std} measured and simulated using equation (7) is shown in Fig. 9. As predicted using equation (7), there is a relationship between the surface resistivity and V_{std}. The three constants K, v_h, and R_b were obtained from the experimental data as K = 1×10^{-12} A/V^2, v_h = 1800 V, and $R_b = 4 \times 10^7$ Ω.

The minimum measurement limit of the probe is dependent on the resistances R_c and R_b; lower R_c and R_b are required for a lower surface resistivity. The maximum measurement limit is also determined by R_c and R_b, although the surface potential of G with a high surface resistivity of 3.0×10^{12} Ω was increased with time, even if the charge eliminator had operated. This is because the traveling motion of the surface charge was so slow due to the high surface resistivity that the charge elimination rate was lower. This rise time of the surface potential can have a linear relationship with the surface resistivity from the result of the rise time measurement [3]. It is suggested that a material with high surface resistivity greater than 10^{12} Ω is also measurable with the same probe configuration as a steady potential measurement.
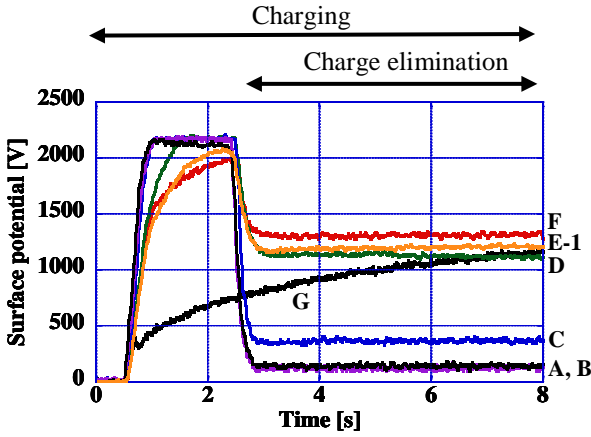
Fig. 7. Surface potential for two samples with different size.
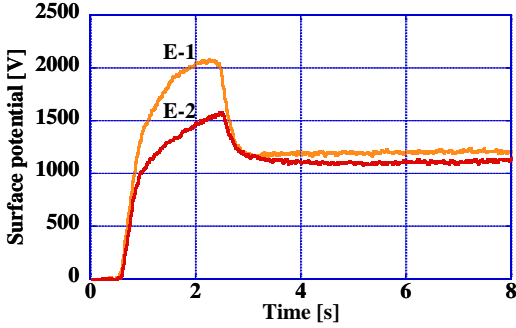
Fig. 8. Surface potential for various surface resistivities.
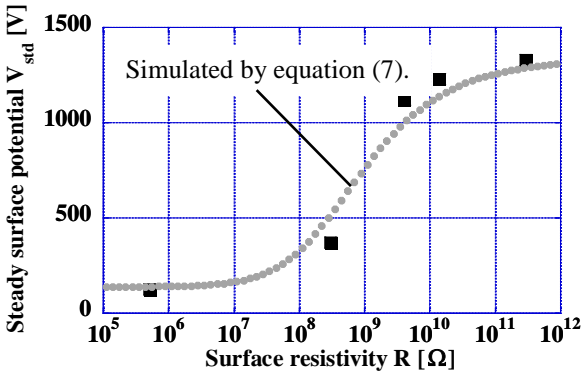
Fig. 9. Steady surface potential V_{std} simulated by eq. (7) and measured experimental results.

REFERENCES

[1] N. Jonassen, "Electrostatics", p. 56, Chapman & Hall, 1998.
[2] International Standard 60093, 1980.
[3] T. Sugimoto and K. Taguchi, "Non-contact surface resistivity measurement for materials greater than 10^9 Ω", *J. Phys. Conf. Ser.*, **646** (2015) 021041.
[4] S. Shahi, A. Bellel, Z. Ziari, A. Kahlouche, and Y. Segui, "Measure and analysis of potential decay in polypropylene films after negative corona charge deposition," *J. Electrostat.*, **57**(2) (2003) 169-181.
[5] *Testing Methods for Electrostatic Propensity of Woven and Knitted Fabrics*, Jpn. Ind. Std., L1094, 1997.
[6] J. N. Chubb, "Instrumentation and standards for testing static control materials," *IEEE Trans. Ind. Appl.*, *26*(6) (1990) 1182-1186.
[7] *Electrostatics—Part 2-1: Measurement Methods—Ability of Materials and Products to Dissipative Static Electric Charge*, Int. Std. IEC 61340-2-1, Jun. 2002.